Journal of Alloys and Compounds 508 (2010) 354–358

Contents lists available at ScienceDirect

Journal of Alloys and Compounds

journal homepage: www.elsevier.com/locate/jallcom

Structure and dielectric behavior of nano-structure ferroelectric $Ba_xSr_{1-x}TiO_3$ prepared by sol–gel method

R.M. Mahani [a], I.K. Battisha [b,*], M. Aly [b], A.B. Abou–Hamad [b]

[a] National Research Center (NRC), Microwave Physics and Dielectrics Dep., Dokky, Egypt
[b] National Research Center (NRC), Solid State Physics Dep., Dokky, Egypt

ARTICLE INFO

Article history:
Received 18 February 2009
Received in revised form 8 May 2010
Accepted 14 May 2010
Available online 27 May 2010

Keywords:
Sol–gel
Dielectric permittivity
Nano-structure $BaTiO_3$
$BaSrTiO_3$

ABSTRACT

Nano-crystalline $Ba_{1-x}Sr_{(x=0.1\text{ and }0.5)}TiO_3$, (B10ST and B50ST) powders have been prepared by sol–gel method, using barium acetate ($Ba(Ac)_2$), titanium butoxide ($Ti(C_4H_9O)_4$), and strontium bromide as precursors. The prepared samples in the form of powder were found to be amorphous, which crystallized to the tetragonal phase after sintering at heat treatment temperature 750 °C in air for 1 h. For the $Ba_{(1-x)}S_{0.1}TiO_3$ powder, which have a crystallite size equal about 33 nm, all major peaks corresponding to perovskite BST phase appeared with (1 1 0) as principle peak. X-ray diffraction (XRD) data were confirmed by transmission electron microscope (TEM). The dielectric measurements were carried out in the frequency range 42 Hz to 1 MHz, at temperature range between 25 °C and 250 °C. The Curie temperature was detected at 125 °C for BT, while it is detected at 110 °C and 75 °C for B10ST and B50ST, respectively. The obtained results showed abrupt decrease in the dielectric permittivity at temperatures above 125 °C and 75 °C, for pure $BaTiO_3$ and $Ba_{0.5}Sr_{0.5}TiO_3$, respectively, leading to phase transition.

1. Introduction

Considerable investigations have focused on ferroelectric materials such as nano-structure barium titanate $BaTiO_3$ (BT) and barium strontium titanate $BaSrTiO_3$ (BST), which are considered to be attractive and advanced material for the electronic industry. This is due to their special dielectric and electro-optics properties. Where BT and BST have high dielectric constant, low dielectric loss, good thermal stability and good high frequency characteristics. The loss factor dissipates or absorbs the incident microwave energy and so insertion loss is decreased when the loss tangent is lower.

BT and BST powders are commonly used for making a number of electronic devices like transducers, piezoelectric actuators, thermal switches, passive memory storage devices and dynamic random access memories (DRAMs), etc. . . [1–12]. The most remarkable property of BT and BST is related to its high dielectric constant, where the room temperature dielectric constant of $BaTiO_3$ ceramics is known to be greater than 2000 [13]. BST finds extensive applications in tunable microwave devices such as filters, varactors, delay lines and phase shifters because of the strong dependence of the dielectric properties on the electric field [14,15].

Several methods have been used for the preparation of BT and BST in powder form. Compared with other techniques, sol–gel method has the advantages of low temperature processing, non-vacuum requirement, low cost [16,17].

This objective work aimed to prepare barium titanate and barium strontium titante in the form of powder in nano-size tetragonal phase, by using sol–gel method. Barium acetate ($Ba(Ac)_2$), titanium butoxide ($Ti(C_4H_9O)_4$), and strontium bromide will be used as the starting materials. The morphology of the prepared samples was evaluated by both transmission electron microscope and scanning electron microscope. TEM micrograph was used to confirm the XRD results. The dielectric properties of pure tetragonal BT and BST were studied as a function of frequency in a wide range of temperatures ranging from 25 °C up to 250 °C.

2. Experimental procedure

2.1. Sample preparation

$BaTiO_3$ (BT), $Ba_{0.5}Ti_{0.5}O_{(3)}$ and $BaSrTiO_3$ (BST), $Ba_{1-x}Sr_{x(x=0.1\text{ and }0.5)}TiO_{(3)}$ (B10ST and B50ST), powders were prepared by a modified sol–gel method. Barium acetate ($Ba(Ac)_2$) (99%, Sisco Research Laboratories PVT. LTD., India) and titanium butoxide ($Ti(C_4H_9O)_4$), (97%, Sigma–Aldrich, Germany) were used as the starting materials; acetyl acetone (AcAc, $C_5H_8O_2$), (98%, Fluka, Switzerland) acetic acid (HAc)-H_2O mixture (96%, Adwic, Egypt) were adopted as solvents of ($Ti(C_4H_9O)_4$), and Ba(Ac)2, respectively. Strontium bromide was added to the precursor with different molar ratios. Densification of gel was obtained, by sintering in air for 1 h at heat treatment temperature 750 °C, in a muffle furnace type (Carbolite CWF 1200).

2.2. Characterization

X-ray diffraction (XRD) patterns from the prepared samples were recorded with a Diano X-ray diffractometer using monochromatized $CoK_{\alpha 1}$ radiation of

* Corresponding author. Tel.: +20 2 25194104.
E-mail address: szbasha@yahoo.com (I.K. Battisha).

0925-8388/$ – see front matter © 2010 Elsevier B.V. All rights reserved.
doi:10.1016/j.jallcom.2010.05.060

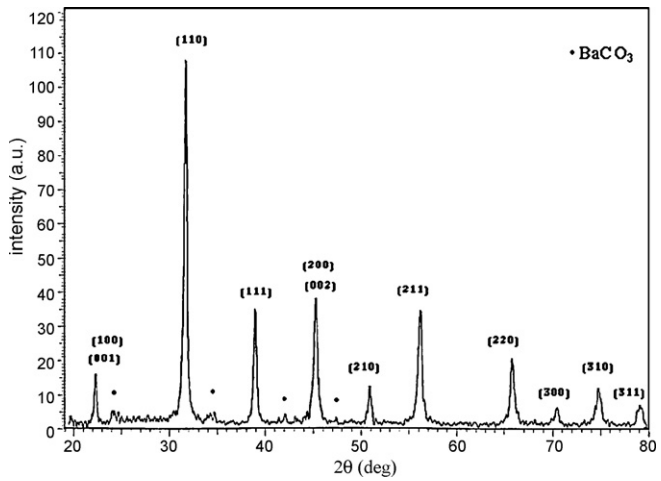

Fig. 1. XRD patterns of pure powder nano-structure BT, sintered at 750 °C for 1 h [17].

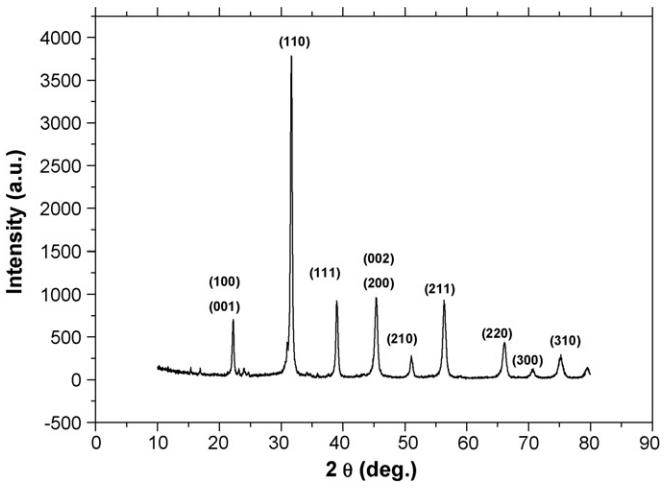

Fig. 2. XRD pattern of B10ST powder sintering at heat treatment temperature 750 °C for 1 h.

wavelength = 1.79026 Å from a fixed source operated at 45 kV and 9 mA. Crystallite sizes G were determined from the Scherrer's equation ($G = \lambda/D\cos\theta$), where λ is the diffraction for a particular Bragg diffraction peak, and D is the (corrected) full width (in radians) of the peak at half maximum (FWHM) intensity.

Microstructure and morphology for the undoped and doped barium titanate were characterized by using the electron microscope of type: "JEOL transmission electron microscope (TEM) model: Jeol 1230" made in Japan magnification power up to 600 k× Resolving power down to 0.2 nm. Accelerating voltage 100 kV, can reach 120 kV through steps.

The computerized LRC bridge (Hioki model 3531 Z Hi Tester) was used to conduct the electrical properties of the investigated samples. The dielectric constant ∈ for the investigated samples was carried out from room temperature up to 250 °C at different frequencies ranging from 42 Hz to 1 MHz. The samples used in the measurement were in the form of disk, have 10 mm in diameter and 3 mm thickness, pressed using a pressure of 10 Tonn, at room temperature.

The relative dielectric permittivity was calculated using the relations:

$$\varepsilon' = \frac{C_m}{C_o}$$
$$\varepsilon'' = \varepsilon' * \tan\delta \quad (1)$$

where C_m is the measured capacitance of the used, C_o is the capacity of the empty condenser.

ε'' is the dielectric loss, $\tan\delta$ is the loss tangent.

The relaxation time was calculated using the relations:

$$\tau = \frac{1}{\omega_m} \quad (2)$$

where $\omega_m = 2\pi f$, f is the frequency.

3. Results and discussion

Fig. 1 shows the X-ray diffraction patterns of pure $BaTiO_3$ (BT) powder, sintered at 750 °C for 1 h. As previously reported in Ref. [17] it is clearly seen that crystallized BT phase can be obtained at heating temperature 750 °C, indicating that one phase tetragonal BT is presented in the prepared BT and BST samples, (referencing to JCPDS files 75-0215 and JCPDS files 79-2265, respectively, for tetragonal phases), which shows well-defined perovskite structure with higher intensity and no detectable secondary phases in the BT pattern [18]. The given data in Table 1 showed that, all the peaks are of tetragonal phase.

The splitting of the (0 0 1) and (1 0 0) doublets confirmed that the prepared powder has a perovskite tetragonal phase in BT sample while this splitting did not appear in B10ST sample which confirms the presence of cubic phase. Unwanted amount of un-

Table 1
$2\theta^\circ$ against the diffraction line of tetragonal phase of pure BT prepared by sol–gel technique in the powder form.

$2\theta^\circ$	Diffraction line of tetragonal phase
22	(1 0 0)
31	(1 1 0)
39	(1 1 1)
45	(0 0 2)
51	(2 1 0)
56	(2 1 1)
70	(2 2 0)
75	(3 0 0)
79	(3 1 0)

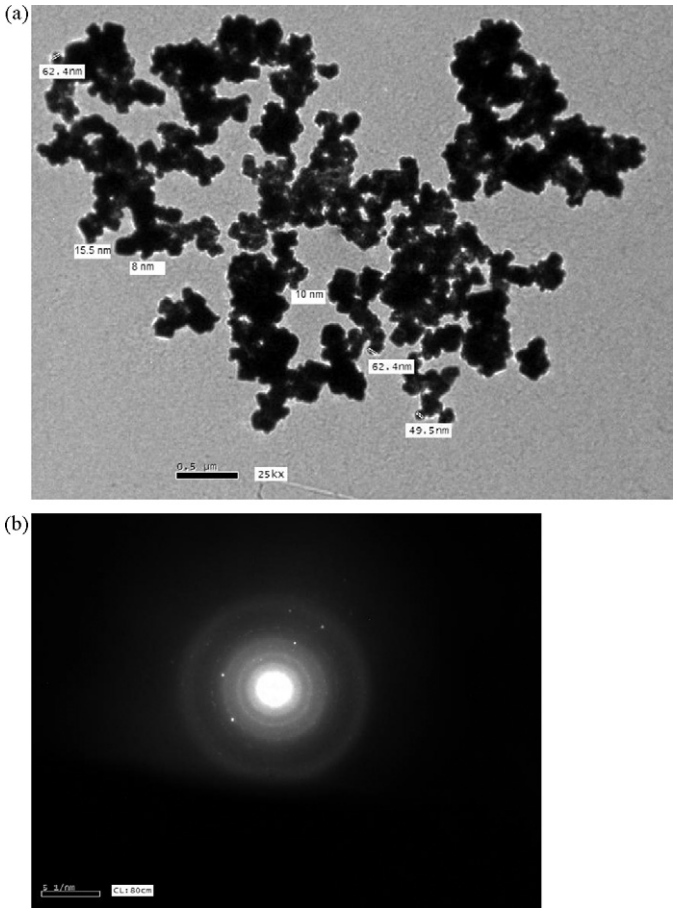

Fig. 3. TEM micrographs (a) and the diffraction pattern (b) of the B10ST powder sample sintered at heat treatment temperature 750 °C for 1 h.

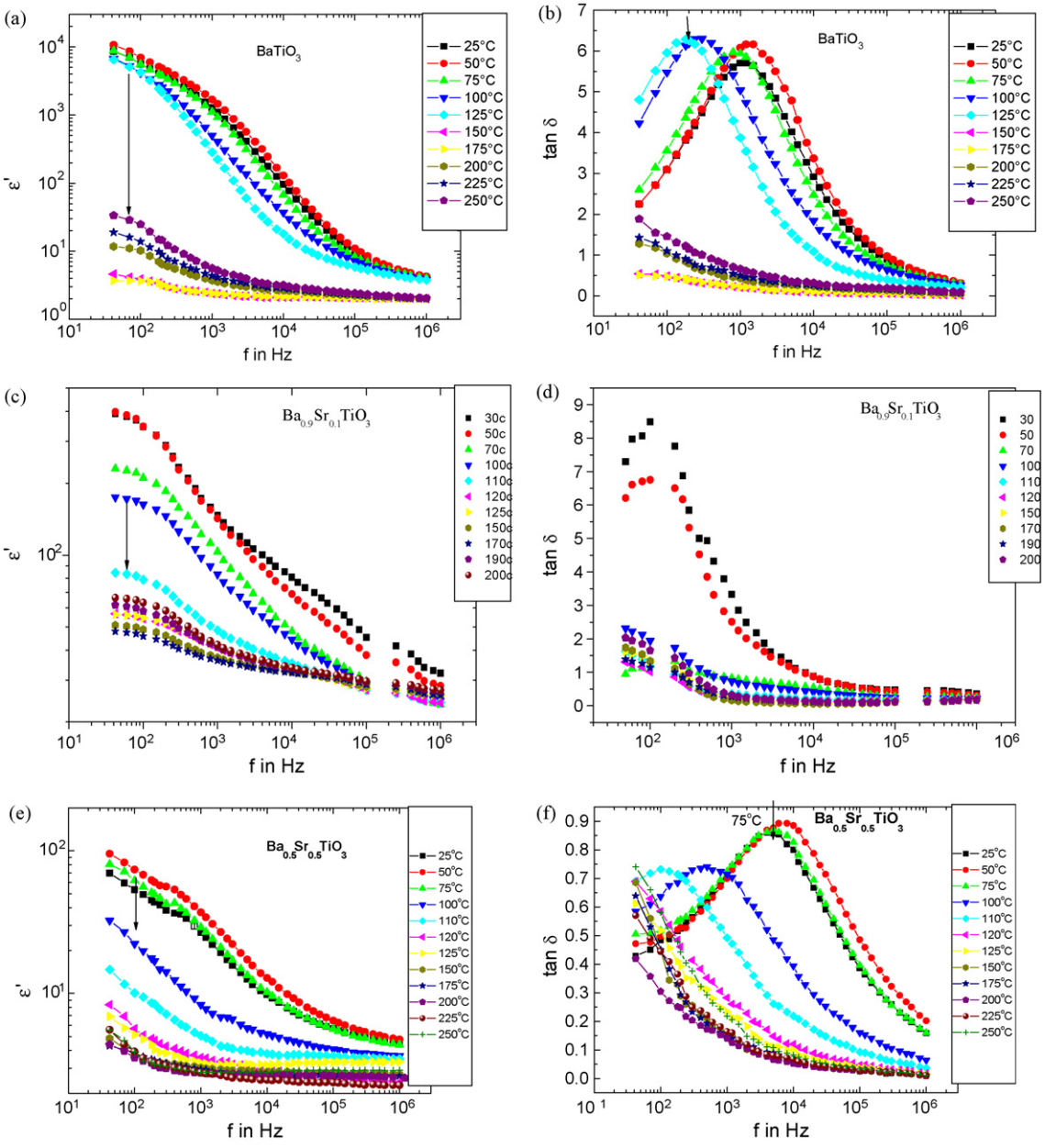

Fig. 4. The frequency dependence of the dielectric permittivity ε' (a, c and e) and the loss tangent tan δ (b, d and f) of BT and B10ST and B50ST. The arrows indicate the Curie temperature.

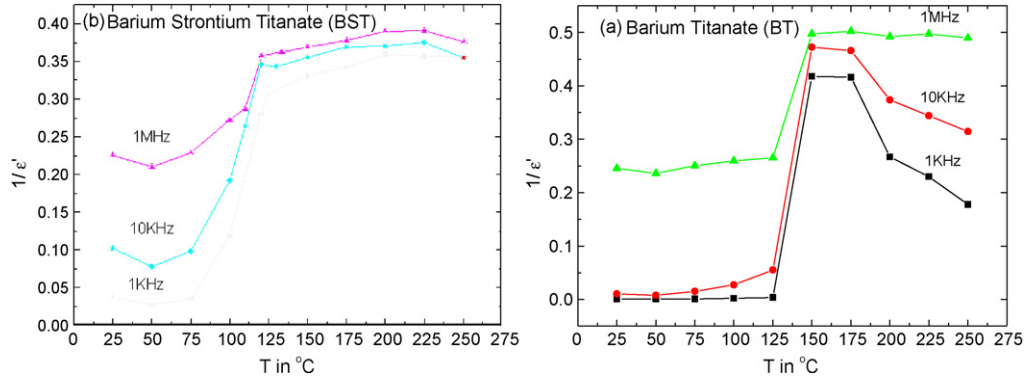

Fig. 5. Values of $1/\varepsilon'$ at various frequencies plotted as a function of temperature for BT and B50ST sintered at 750 °C for 1 h.

reacted $BaCO_3$ (By reference to JCPDS files 45-1471 for Witherite, syn) resulting from the reaction of BaO with atmospheric CO_2 and the burn-out of organic materials or as a result of incomplete calcinations appeared in Fig. 1.

Fig. 2 shows the X-ray diffraction pattern of the B10ST powder annealed at 750 °C, which shows all major bands corresponding to perovskite BST phase with (1 1 0) as the major peak [20].

The accurate crystallite sizes were calculated by using the full width at half maximum of the main (1 1 0) diffraction peak using the Scherrer's equation and confirmed by using the WinFit program for both BT and B10ST samples. The calculated crystallite sizes were found to be 39.5 and 33 nm for BT and B10ST, respectively. Based on these results, it should be noted that the average particle size was significantly reduced by Sr doping.

The properties and morphology of the B10ST powder can be explained on the basis of the microstructure, as shown in Fig. 3a and b. TEM image of B10ST powders sintered at 750 °C is illustrated in Fig. 3a. While the selected-area electron diffraction (SAED) patterns obtained from the TEM of the same sample is shown in Fig. 3b. The (SAED) patterns indicate that the prepared samples are assigned to perovskite phase [19]. The grain size was determined by averaging over the total number of crystallite size in the TEM (Jeol1230) micrograph. Based on this method, the average crystallite size of B10ST powders, synthesized by sol–gel method, was 34.6 nm, which is larger than the XRD results, probably resulting from the fact that the uniform strain within the particles that would lead to the line broadening in XRD pattern were not taken into account [21].

Fig. 4a and b shows the dielectric permittivity (ε') and the loss tangent ($\tan\delta$) of pure barium titanate (BT) as a function of frequency, during heating in the range starting from 25 °C up to 250 °C. From the preceding figures the Curie temperature was detected at 125 °C for BT. While it is detected at 110 °C and 75 °C for B10ST and B50ST, respectively, as shown in Fig. 5c–f, which shows the dielectric permittivity and loss tangent, of the barium strontium titanate system B10ST and B50ST, respectively.

It is clear from Fig. 4a and b that ε' decreased with increasing frequency showing an anomalous dispersion. Such dispersion in ε' is accompanied by a relaxation peak in $\tan\delta$; see Fig. 4b. The intensity of this peak slightly increased and its maximum shifted to lower frequencies with increasing temperatures, then, it disappeared at temperature above 125 °C.

Abrupt decrease in ε' is observed at temperature above 125 °C, leads to a phase transition. Such transition occurred at definite temperatures called Curie temperature (T_c), at which BT transformed from the ferroelectric phase (polarized state) to the para-electric phase (unpolarized sate). Large values seen in the dielectric permittivity at certain temperature range between room temperature and 125 °C, in which the ferroelectricity property is dominated. Thus, the permanent dipole moment dominated polarization which in turn affects the dielectric permittivity arises from the displacement of negatively charged oxygen ions and positively charged titanium ions from their symmetrical positions (upward displacement). As a result, an elongation in the vertical direction can be occurred leading to tetragonal phase. So, the dielectric behavior of barium titanate in the tetragonal phase is in good agreement with that characterized by XRD, see Fig. 1.

On the other hand, by heating BT above its Curie temperature (T_c), both ε' and $\tan\delta$ markedly decreased. This is because the formed tetragonal phase (non-symmetric) at lower temperature transformed into cubic phase (symmetric) at temperature higher than T_c [20]. In this case, the formed crystalline phase of BT is para-electric which has no permanent dipole moment and in turn it behaves like dielectric.

For the barium strontium titanate system B10ST and B50ST, no significantly changes can be observed in the dielectric permittivity and loss tangent at temperatures lower than 110 and 75 °C, see Fig. 4c–f for B10ST and B50ST, respectively. But above those temperatures, both of them markedly decreased. So, 110 °C and 75 °C represent the Curie temperature of both of the barium strontium titanate system, see the vertical arrows on the presented plots shown in Fig. 4c–f. The decrease in ε' with increasing frequency results in a relaxation peak in $\tan\delta$. The maximum of this peak decreased and shifted to lower frequencies with increasing temperature and then disappeared at temperature above 110 °C. However, the abrupt decrease in the intensity of this peak is indicated at temperature above 75 °C for B50ST.

Table 2
The temperature dependence of ε' and $\tan\delta$ for BT and B50ST at 1 kHz.

T in °C	BT		B50ST	
	ε'	$\tan\delta$	ε'	$\tan\delta$
25	1282	5.70	26	0.72
50	1692	6.08	37	0.70
75	1111	5.93	29	0.73
100	504	5.04	8.2	0.71
125	285	3.87	3.2	0.23
150	2.4	0.20	3.0	0.15
175	2.4	0.21	2.9	0.14
200	3.7	0.43	2.8	0.14
225	4.3	0.50	2.8	0.16
250	5.6	0.66	2.8	0.22

The comparison between the dielectric behavior of BT and barium strontium titanate system B50ST prepared in the nano-size, is clear from the large differences in their dielectric permittivities measured as a function of frequency and at different temperatures, see Table 2. It is evident from this table that the dielectric permittivity of BT largely decreased on doping it with strontium bromide. This is because strontium titanate is usually used to maintain relativity low temperature dependence of the dielectric permittivity [21]. In addition, such decrease may be related to the fact that strontium titanate has different lattice constant which add a stress into the lattice.

In order to observe clearly the Curie temperature for BT and B50ST, we plotted the inverse of the dielectric permittivity as a function of temperature at 1 kHz, 10 kHz and 1 MHz as shown in Fig. 5. In this figure, BT shows abrupt increase in its $1/\varepsilon'$ (decrease in ε') at temperature above 125 °C under the mentioned frequencies. While for B50ST, the abrupt increase in $1/\varepsilon'$ is seen at temperature above 75 °C. This means that the Curie temperature of pure BT is observed at lower temperature on doping it with strontium bromide. This is might be due to that the strontium titanate is usually employed to lower the Curie point [22]. However, the rate of

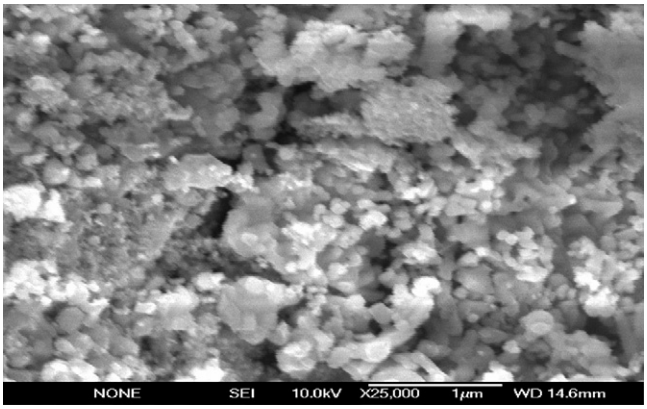

Fig. 6. The SEM micrograph of B10ST powder sample sintering at heat treatment temperature 750 °C for 1 h.

increase in inverse permittivity for BT is sharper than that obtained for B50ST.

SEM micrograph image of (B10ST) powders both sintered for 1 h at 750 °C is illustrated in Fig. 6. These images show grains typical of BST powder, which consists of a granular microstructure with irregular shaped grains.

Some degrees of agglomeration in this powdered sample, and the clusters consisted of several small grains. The particles of the sample have a well-defined shape. This is might be due to some aggregates of particles together.

4. Conclusion

Using the sol–gel method, nano-crystalline pure $BaTiO_3$ (BT) and B10ST and B50ST powders have been successfully prepared. Under the investigated experimental conditions, single tetragonal phases have been obtained for pure sample and also a well-defined tetragonal perovskite phase of BT with crystallite sizes = 39.5 nm was appeared, which decreases to 33 nm by doping with Sr in B10ST samples. TEM micrograph was used to confirm the XRD results, where the crystallite size calculated from TEM for the B10ST was in nano-scale and equal to 34.6 nm. The dielectric properties of both BT and BST systems in the ferroelectric phase showed strongly frequency and temperature dependence. Also, dielectric properties showed that Curie temperature of BT shifted to lower temperature on doping it with strontium bromide.

References

[1] A. Sundaresan, C.N.R. Rao, J. Nano Today 4 (2009) 96.
[2] L.B. Kong, T.S. Zhang, J. Ma, F. Boey, J. Prog. Mater. Sci. 53 (2008) 207.
[3] F. Mouraa, A.Z. Simões, B.D. Stojanovic, M.A. Zaghete, E. Longo, J.A. Varela, J. Alloys Compd. 462 (2008) 129.
[4] I.K. Battisha, A.A. Hamad, R.M. Mahani, Physica B 404 (2009) 2274.
[5] H.I. Hsiang, C.S. Hsib, C.C. Huang, S.L. Fu, Mater. Chem. Phys. 113 (2009) 658.
[6] P. Yu, B. Cui, Q. Shi, Mater. Sci. Eng. A 473 (2008) 34.
[7] C. Mao, X. Dong, T. Zeng, H. Chen, F. Cao, Ceram. Int. 34 (2008) 45.
[8] R. Kavian, A. Saidi, J. Alloys Compd. 468 (2009) 528.
[9] W. Li, Z. Xu, R. Chu, P. Fu, J. Hao, J. Alloys Compd. 482 (2009) 137.
[10] W.L. Liu, D. Xuea, H. Kanga, C. Liu, J. Alloys Compd. 440 (2007) 78.
[11] B. Fournaud, S. Rossignol, J.M. Tatibou, S. Thollonb, J. Mater. Process. Technol. 209 (2009) 2515.
[12] L.B. Kong, T.S. Zhang, J. Ma, F. Boey, Prog. Mater. Sci. 53 (2008) 207.
[13] M.S. Zhang, J. Yu, W.C. Chen, Z. Yin, Prog. Cryst. Growth Charact. Mater. 40 (1–4) (2000) 33.
[14] H.-D. Wu, F.S. Barnes, Integr. Ferroelectr. 22 (1998) 291.
[15] Y.-A. Jeon, E.-S. Choi, T.-S. Seo, S.-G. Yoon, Appl. Phys. Lett. 79 (2001) 1012.
[16] A.G.A. Darwish, Y. Badr, M. El Shaarawy, N.M.H. Shash, I.K. Battisha, J. Alloys Compd. 489 (2010) 451.
[17] I.K. Battisha, Y. Badr, N.M. Shash, M.G. El–Shaarawy, A.G.A. Darwish, J. Sol–Gel Sci. Technol., published online 27 January 2010, LLC 2010, doi:10.1007/s10971-009-2129-5.
[20] M. Nayak, T.Y. Tseng, J. Thin Solid Films 408 (2002) 194.
[21] X. Wei, G. Xu, Z. Ren, Y. Wang, Ge Shen, G. Han, Mater. Lett. 62 (2008) 3666–3669, 3667.
[22] I.K. Battisha, A.B. Abou Hamad, R.M. Mahani, Physica B 404 (2009) 2274–2279.